HEFAT2010
7th International Conference on Heat Transfer, Fluid Mechanics and Thermodynamics
19-21 July 2010
Antalya, Turkey

EXPERIMENTAL AND THREE-DIMENSIONAL NUMERICAL INVESTIGATION OF LAMINAR FLOW HEAT TRANSFER IN A RECTANGULAR DUCT UNDER UNIFORM BOTTOM SURFACE TEMPERATURE WITH DEVELOPING VELOCITY AND TEMPERATURE FIELDS

Arslan K., Onur N.* and Turgut O.
*Author for correspondence
Department of Mechanical Engineering,
Faculty of Engineering and Architecture,
University of Gazi,
06570 Maltepe, Ankara,
Turkey,
E-mail: nevonur@gazi.edu.tr

ABSTRACT

In this study, steady-state laminar forced convection heat transfer in a horizontal smooth rectangular duct was investigated both experimentally and numerically in the Reynolds number range of 295 to 2019. Velocity and temperature distribution begin to develop simultaneously in the heated section. A constant temperature boundary condition was applied on bottom surface of the duct. A commercial CFD program Ansys Fluent 6.3.26 was used to carry out the numerical study. Based on the present experimental and numerical study, new engineering data were presented for the heat transfer and friction coefficients. The maximum relative uncertainties are estimated to be 2.83 and 3.11 % for average Darcy friction factor and average Nusselt number, respectively. It is seen that there is a good agreement between the present experimental and numerical results.

INTRODUCTION

Predicting the pressure drop and heat transfer under developing flow conditions is quite important in many applications such as compact heat exchangers where flow passages are typically short in length. Laminar flow and heat transfer in rectangular channels have received considerable attention due to their practical importance. Especially, laminar forced convection inside ducts is of interest in the design of a low-Reynolds number heat exchanger apparatus. Ducts having rectangular cross-sections are widely used in industrial heat transfer equipments such as compact heat exchangers. These devices are required to be compact as well as to transfer heat rapidly to the environment. Among the various duct cross sections, a rectangular duct is used in compact heat exchanger extensively, because of its simplicity of construction.

Several studies of laminar flow in straight rectangular ducts have been presented in the past. An excellent comprehensive review of laminar flow forced convection in rectangular ducts was presented by Shah and London [1], Kakaç et. al [2], and Kakaç and Liu [3]. Zhang [4] analyzed numerically hydrodynamically developed thermally developing forced convection heat transfer in rectangular duct under uniform plate temperature. Bottom and top plates of the rectangular duct were kept at constant temperature, at the same time different conductance materials were chosen for side walls. Various duct aspect ratios were considered, and the side walls had different conductance parameters from 0 to infinitely large. Muzychka and Yovanovich [5] investigated laminar combined developing flow in non-circular ducts. New models were proposed which simplify the prediction of the Nusselt number for combined entry region in most non-circular duct geometries. This new model predicts both local and average Nusselt numbers and is valid for both isothermal and isoflux boundary conditions. Chung et al. [6] investigated numerically behavior of hydrodynamically fully developed and thermally developing laminar flow of Newtonian fluids in rectangular ducts for the constant heat flux boundary condition. The developing Nusselt number was obtained for a wide range of duct aspect ratios. Aparecido and Cotta [7] analytically studied laminar forced convection inside rectangular duct by extending the generalized integral transform technique. Fully developed and thermally developing regions were examined. Beavers et al. [8] investigated experimentally hydrodynamically developing laminar flow in rectangular ducts for different aspect ratio. The concern of the research is the determination of the pressure field associated with the hydrodynamic development of the flow in rectangular duct. Montgomery and Wibulswas [9] developed an alternative numerical method which is used to solve the heat transfer equations for laminar flow in ducts of rectangular cross section with simultaneously developing temperature and velocity profiles, both for constant wall temperature and for constant heat input per unit length of the duct. Comparisons of analytical solutions for circular ducts and

parallel plates were made with experimental data. It was observed that Prandtl number had a strong effect on the Nusselt number for simultaneously developing velocity and temperature profiles. Sparrow [10] studied the laminar simultaneous development of temperature and velocity profiles in the entrance region of a flat rectangular duct for different Prandtl numbers Two temperature conditions at the duct walls were considered: both duct walls had the same uniform temperature and one of the duct walls was maintained at a uniform temperature while the other wall was insulated. The results were given graphically for different boundary conditions for various Reynolds number and Prandtl numbers. Savino and Siegel [11] determined the temperature distributions analytically for fully developed laminar heat transfer in rectangular ducts with different aspect ratios. The channel walls were uniformly heated, but the heat flux on the short sides was an arbitrary fraction of the heat flux on the broad sides.

The present study concerns experimental and three dimensional numerical study of laminar flow in a bottom surface isothermally heated horizontal straight rectangular duct under hydrodynamically and thermally developing flow conditions. Air ($Pr \cong 0.7$) is used as the heat transfer medium. The momentum, continuity and energy equations for three dimensional laminar flow in the hydrodynamic and thermal entrance region of rectangular channels are solved using finite volume based commercial software Ansys Fluent 6.3.26. Practical engineering correlations for the average Nusselt number and average Darcy friction factor are also determined.

EXPERIMENTAL PROGRAM

A schematic diagram of the experimental apparatus with appropriate dimensions used in the experiments is illustrated in Figure 1a. The test facility described below is a fully instrumented capable of providing steady-state flow rates of air at well-controlled conditions. The test facility used for the experiments was operated in the open circuit mode over a velocity range which gave rise to duct hydraulic diameter based Reynolds numbers ranging from 295 to 2019 with air being drawn from the laboratory room. The present experiments are undertaken to investigate in depth to study the heat transfer and fluid flow characteristics in a duct having rectangular cross-section under hydrodynamically and thermally developing laminar flow conditions. Experimental set-up basically consists of two rectangular cross-sectioned ducts, a radial fan, and a circular-sectioned duct, and all of which are connected in series. Rectangular cross-sectioned duct assembly consists of two consecutive parts: a 50.8 cm in length test section and a 50.8 cm in length exit section. These two sections, fabricated from wood 0.02 m in thickness, have identical internal cross-sectional shape and dimensions. The copper plate was located at the bottom surface of the test duct, in order to obtain constant surface temperature. Cross-section of the rectangular duct and its dimensions are displayed in Figure 1b. The hydraulic diameter of the duct is 0.075 m. A plexiglass gasket was placed between sections for insulation purposes. Flow straighter was located at the inlet of the test section of test facility to obtain uniform flow conditions. A fine screen was placed in front of the flow straighter. Initial studies indicated that flow was uniform and steady. Air from the laboratory room is drawn into the test section. In other words, hydrodynamically and thermally developing laminar flow enters the test section. This means that the velocity and temperature of the fluid is uniform over the flow cross section at the inlet of the test section. The bottom surface of the test section is kept at a constant temperature. Other three surfaces were insulated. This type of problem is called combined hydrodynamic and thermal entry length problem [12]. To minimize the exit effects of test section, another rectangular cross-sectioned duct is used after the test section. The surfaces of the exit section were insulated. Air in laboratory room is sucked into the rectangular duct by the radial fan, at 1.5 kW, which is installed at the outlet of the rectangular exit section of the test facility. The fan is physically isolated from the exit duct using flexible connecting nylon tube to inhibit the transmission of vibration. The fan outlet is connected to a circular pipe whose entire length and diameter are 4.5 m and 0.072 m, respectively. Ratio of the circular duct length-to-diameter is chosen to ensure that fully developed flow is achieved in the circular duct before the velocity measurements are taken.

Accurate temperature measurements were necessary and for this reason all temperatures were measured using fiberglass-insulated 30 gauge T-type copper-constantan thermocouples. All the thermocouples used in temperature measurements have the same accuracy. Each thermocouple was calibrated individually before experiments. The measured temperatures were used to obtain the average air and surface temperatures at appropriate locations in order to calculate the average Nusselt number. In order to determine the surface-temperature distribution along the length of the test-section, the thermocouples were located at the bottom of the test section as shown in Figure 2a. The spot-welded thermocouple is embedded in a narrow hole of the surface, which is perpendicular to the air-flow direction. A heat transfer compound (Arctic Silver Thermal Adhesive) is applied to fill the residual cavity between the thermal junction and the surface to ensure a good thermal contact. This method enabled the point of measurement to be placed closer to the inner surface of the surface, where the temperature reading is more desirable, and more accurate temperature measurements will be made [13].

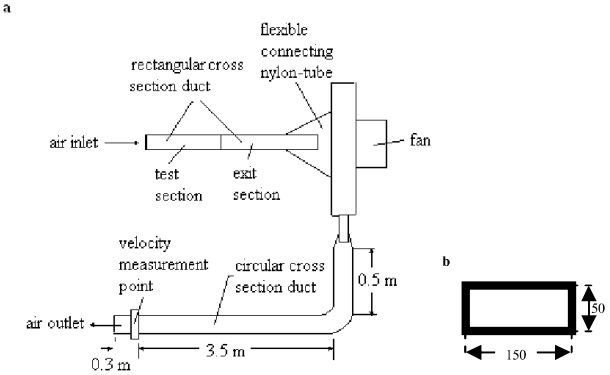

Figure 1 (**a**) Schematic diagram of the experimental set-up; (**b**) duct cross-section (dimensions in mm)

As shown in Figure 2b and Figure 2c, two planes perpendicular to the main direction of the air flow are chosen for air temperature measurements at the inlet and exit of the test duct. To measure the steady-state temperatures of the air flow at the inlet and outlet of the test section, eight thermocouples were placed as shown in Figure 2b and Figure 2c. Two static pressure taps are also located at the same cross-sections where the inlet and outlet air temperatures are measured in the test section to measure the pressure drop Δp across the test section. The pressure taps are 0.0024 m in diameter as recommended by Benedict [14]. Flexible electric heater is located under the bottom surface of the test section. It is determined experimentally that the resistance of heating element is found to be constant for temperature range of the experiment. Variable electric power was available from separate voltage source. Temperature measurements indicated that the variation of temperature on bottom surface of the test section along the flow direction is negligible. Average surface temperature is determined from these temperature readings.

The heat transfer to the ambient environment is minimized by insulation. For this reason, as it can be seen in Figure 3, the bottom surface of the test section are thermally insulated starting from its surface by applying a 0.04 m in thickness fiberglass, 0.04 m in thickness insulation foam and 0.02 m in thickness wooden plate. Also, all the surface of the test duct and exit duct were insulated with 0.04 m. insulated foam. All of the junctions in experimental apparatus were covered with transparent silicone to prevent air leakage from junction to ambient.

In order to evaluate the conduction heat loss from the test section, thermocouples are also located at appropriate positions along the flow direction to the inside and outside surface of the insulation foam. The ambient air temperature is also monitored by a thermocouple.

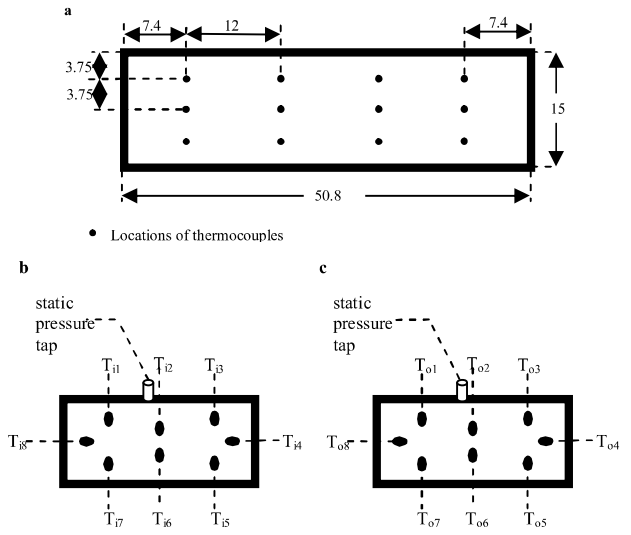

Figure 2 (**a**) The locations of the thermocouples used measuring surface temperature along flow direction in bottom surface of the test section (dimensions in cm); the location of the static pressure tap and thermocouples used measuring the air temperature (**b**) at inlet and (**c**) at outlet

Error in temperature, length, pressure, velocity, and electrical measurements are ±0.3 °C, ±0.1 mm, ±2 %, ±1 %, and ±0.5 %, respectively. So for the Reynolds number *Re*, average Darcy friction factor *f*, and average Nusselt number Nu_m, following the procedure described by Holman [15], the maximum relative uncertainty are estimated to be 1.02 %, 2.83 %, and 3.11 %, respectively.

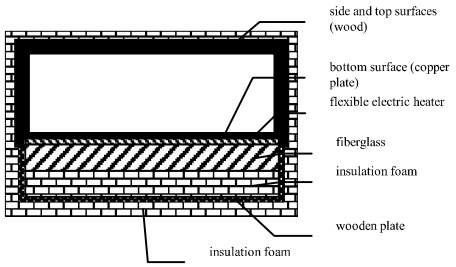

Figure 3 The locations of the insulation materials of the test section

During a typical experiment, a predetermined power input was supplied by variac. The air velocity near the outlet of the circular pipe was measured. Velocity measurements were taken at seven different locations in the same plane, with an even interval of 0.006 m along the pipe radius, away from its centre line. According to the principle of mass conservation, the mass flow rate of air through the circular pipe is equal to that passing through the rectangular duct. Then the system was allowed to reach thermal equilibrium. This required approximately four to five hours. After thermal equilibrium was reached, data was collected.

The basic energy balance for a duct flow, under steady-state conditions are given as:

$$Q_c = E - Q_l - Q_r \qquad (1)$$

Electrical power supplied to heat the bottom surface of the rectangular test duct is denoted by E [W]. The amount of conduction heat loss from the test duct to the ambient air Q_l [W] is estimated by one dimensional heat transfer analysis using the Fourier's law and from the knowledge of the thermal conductivity (0.027 W/m K) of the insulation foam and the measured temperatures. The rate of radiative heat loss Q_r [W] through the test duct is estimated by the Stefan Boltzman law [13].

After Q_l and Q_r (which are less than approximately 3.5 and 4.3 % of total electric power input E, respectively) are deducted from total electric power input E to estimate the value of convective heat transfer Q_c to air flowing in the rectangular duct. Then the average convective heat transfer coefficient of the air flow in the rectangular duct is obtained [16] as follows

$$h_m = Q_c / A(T_w - T_b) \qquad (2)$$

where A [m^2] is the surface area (i.e. in contact with the air) of the bottom surface of the test section, T_w [K] is the surface temperature of the bottom surface of test-section duct, and T_b [K] is the mean bulk temperature of the air flow of the test section. The hydraulic diameter of the rectangular duct is defined by $D_h=4A_c/P$ where A_c [m^2] is the cross sectional area and P [m] is the wetted perimeter. The hydraulic diameter is chosen as the characteristic dimension to define the Reynolds number and average Nusselt number, i.e.

$Re=UD_h/\nu$ (3)

$Nu_m=h_mD_h/k$ (4)

In equations (3) and (4), U [m/s] is the mean velocity of the air flow in the rectangular duct, ν [m^2/s] is the kinematic viscosity of air, and k [W/m K] is the thermal conductivity of air.

For the temperature range considered in the experiments, Prandtl number, Pr, of air remained almost constant at a value of 0.7. Hence, average Nusselt number in the rectangular duct is depicted as given below:

$$Nu_m = C_1 Re^{n_1} \quad (5)$$

One of the key parameters of interest in the thermal entrance region is average Darcy friction factor f. The friction factor along the channel is traditionally expressed in terms of pressure drop and average velocity in the following form

$f=\Delta p(D_h/L)/(\rho U^2/2)$ (6)

Here Δp [Pa] is the pressure drop along the test section, L [m] is the axial length of the test-section, and ρ [kg/m] is the density of air. Furthermore, the following form is assumed for Darcy friction factor in laminar flow rectangular duct following the line of reasoning as suggested by Blasius [17]:

$$f = C_2 Re^{n_2} \quad (7)$$

In equations (5) and (7), C_1 and C_2 are constant coefficients; n_1 and n_2 are power indices. All fluid properties in the test section are evaluated at the bulk temperature $T_b=(T_{bi}+T_{bo})/2$ where T_{bi} [K] and T_{bo} [K] are the bulk temperatures of the air at the inlet and outlet of the test section, respectively. The air flow properties are taken from Incropera and DeWitt [18].

THEORETICAL DESCRIPTION

Figure 4a denotes the computational domain of the test section along with the coordinate system and flow geometry. This arrangement is the same as the one employed for the present experimental study. Test section is mathematically modeled for numerical computations. Since the flow field is symmetric with respect to y-x plane, only one half of the channels has been considered for computational domain to reduce the computation domain.

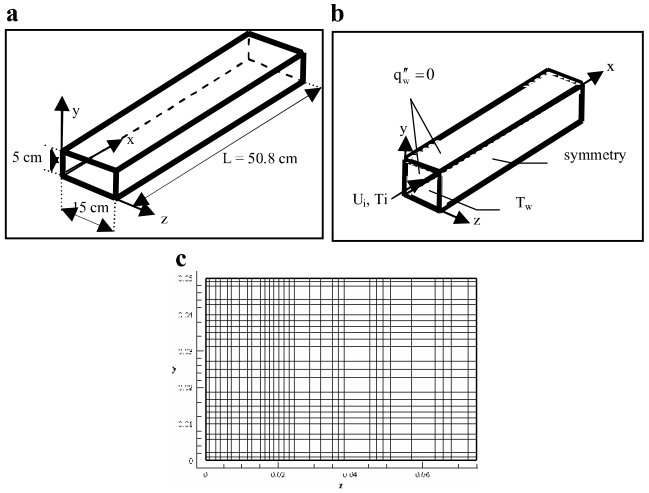

Figure 4 (**a**) Computational domain of the test section, (**b**) boundary condition of the test section; (**c**) mesh distribution in y-z plane

The three dimensional steady laminar constant property viscous flow enters the test section. The principle flow is in the x-direction. The flow is governed by the usual continuity, momentum and energy equations as follows

$$\vec{\nabla}\cdot\vec{V} = 0 \quad (8)$$

$$\rho\frac{D\vec{V}}{Dt} = -\nabla p + \mu\nabla^2\vec{V} \quad (9)$$

$$\rho c_p\frac{DT}{Dt} = k\nabla^2 T \quad (10)$$

where $\vec{V}$ [m/s] is the velocity vector, μ [kg/m s] is the dynamic viscosity, T [K] is the temperature, and c_p [J/kg K] is the specific heat.

Flow enters the test section with uniform velocity and temperature profile. The principle flow is in the x-direction. In the test section, the laminar and steady constant-property three-dimensional incompressible Newtonian viscous flow with negligible buoyancy effects and viscous dissipation is assumed. The physical properties of fluid, taken at the bulk temperature, have been considered to be constant for the test section. No slip boundary conditions were employed on the duct walls. At the outlet of the test section, pressure outlet boundary condition of Ansys Fluent 6.3.26 was used. Symmetry boundary condition was employed on the symmetry plane. A uniform wall temperature boundary condition is employed on the bottom surface of test section. Insulated boundary condition was applied on the side and top surfaces of test duct. All the boundary conditions applied on the test duct were depicted in Figure 4b.

In this study, a general purpose finite-volume based commercial CFD software package Ansys Fluent 6.3.26 has been used to carry out the numerical study. The code provides mesh flexibility by structured and unstructured meshes.

Computations are performed for laminar flow conditions. The energy equation is solved neglecting radiation as well as viscous dissipation effects. In the present study, hexahedral cells are created with a fine mesh near the walls using a preprocessor called Ansys Gambit 2.3. A non-uniform grid distribution is employed in the plane perpendicular to the main flow direction while uniform grid distribution is employed in main flow direction. Grid distribution in y-z plane is depicted in Figure 4c. Close to each wall, the number of grid points or control volumes is increased to enhance the resolution and accuracy. Steady segregated solver is used with second order upwind scheme for convective terms in the mass, momentum, and energy equations. For pressure discretization, the standard scheme has been employed while the SIMPLE-algorithm has been used for pressure-velocity coupling discretization.

To assure the accuracy of the results presented, a grid independence study is carried out to study the effects of grid size using eight different grid sizes changing from 100x10x15 to 387x38x57 in the x-, y-, and z-coordinate directions for Re=2019. It is observed that further refinement of grids from 320x32x48 to 352x35x52 did not have a significant effect on the results in terms of average Nusselt number and average Darcy friction factor (variation in both average Nusselt number and average Darcy friction factor were less than 0.14 % and 0.42 %, respectively). Based on this observation, a uniform grid

of 320x32x48 points is chosen. No convergence problems are observed. This optimum grid is also used for other Reynolds numbers. To obtain convergence, each equation for mass and momentum has been iterated until the residual falls below $1x10^{-5}$ while energy equation has been iterated until the residual falls below $1x10^{-6}$.

RESULTS AND DISCUSSION

In the study reported here, the laminar convective heat transfer and fluid friction in an air-cooled rectangular cross-section under uniform bottom surface temperature is both experimentally and numerically investigated. The investigation is carried out under hydrodynamically and thermally developing flow conditions. The average Nusselt numbers and average Darcy friction factor are estimated in this study. Experimental and numerical results are presented in Figure 5 through Figure 8. Plotted in these figures are the best-fit lines in the forms suggested by equations (5) and (7).

The velocity and temperature fields at different axial locations along the channel are considered first. Typical velocity magnitude contours at x=0.1, 0.3, and 0.508 m (outlet of the test section) are presented in Figure 5 for Re=2019. It is seen from Figure 5 that maximum velocity occurs in the center of the duct. Typical temperature contours at x=0.1, 0.3, and 0.508 m (outlet of the test section) are also depicted in Figure 6 for Re=2019.

In order to show that whether the flow is hydrodynamically fully developed at the outlet of the test section, typical velocity profiles at symmetry plane (see Figure 4) for at x=0.1m, x=0.3m, x=0.5m and the exit of the duct are shown in Figure 7a for Re=2019. As can be seen from Figure 7a, the velocity magnitude profile at different location along x-direction in the rectangular duct is plotted as a function of the dimensionless height y/H of the duct. In the fully developed region, the velocity profile repeated itself at various positions along the duct. As it can be seen from Figure 7a, velocity distribution for flow is reached nearly hydrodynamically fully developed flow condition at the exit of the test section.

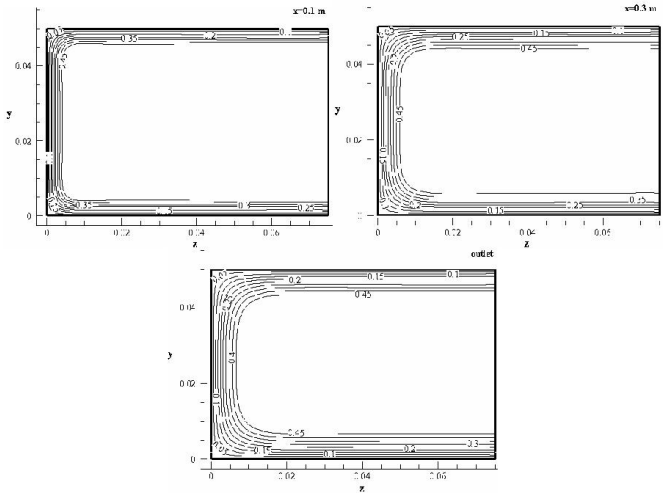

Figure 5 Isovel contours of velocity magnitude at x=0.1, 0.3 and 0.508 m (outlet of the test section)

Dimensionless temperature profile is defined as $\Theta=(T_w-T(x,y,z))/(T_w-T_i)$ where T_w [K] is the bottom wall temperature of the test section and T_i [K] is the inlet temperature [2]. A plane is defined at the symmetry plane in order to see the variation of dimensionless temperature profile along the duct. Dimensionless temperature distribution is plotted as function of the dimensionless height y/H of the duct for various positions along the duct on this plane. Dimensionless temperature distribution on this plane along the test section for at x=0.1m, x=0.3m, x=0.5m from the inlet section and the exit of the test duct are depicted in Figure 7b. It is clearly obtained that dimensionless temperature distribution is reached nearly thermally fully developed conditions at the exit of the test section.

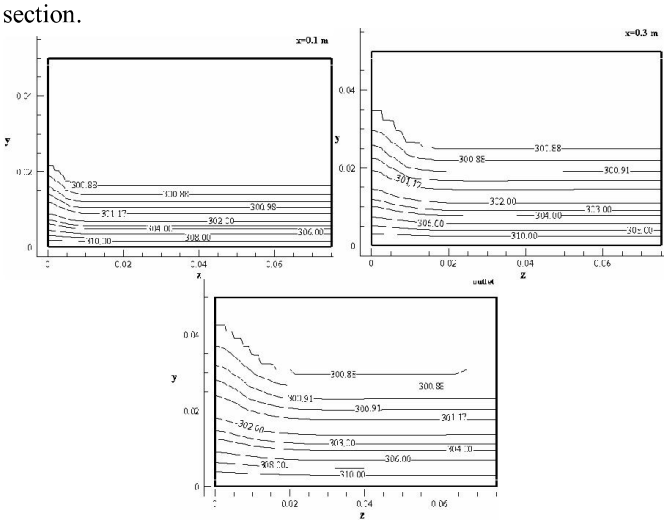

Figure 6 Temperature contours at x=0.1, 0.3 and 0.508 m (outlet of the test section)

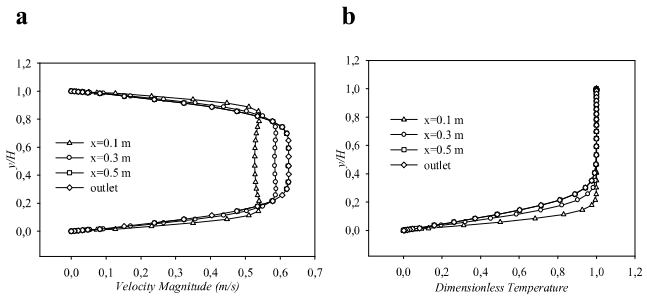

Figure 7 Velocity (**a**) and dimensionless temperature (**b**) distribution on symmetry plane at along with the test section

Figure 8a and Figure 8b display the experimental and numerical values of average Nusselt number and average Darcy friction factor for the test section, respectively.

After examination of the Figure 8a and Figure 8b, it can be seen that experimental and numerical results show a very good agreement. The results have shown that as the Reynolds number increases, heat transfer coefficient increases as expected. In addition, Darcy friction factor decreases with increasing the Reynolds number.

In order to provide a single equation for average Nusselt number representing data, the variation of experimental Nusselt number as a function of Reynolds number is given as follows:

$$Nu_{m,experimental}=0.3620Re^{0.4636} \quad (11)$$

The maximum deviation from the best-fit line for equation (11) is within ±5 %.

Similarly numerically obtained average Nusselt number is presented as a function of Reynolds number and presented as given below:

$$Nu_{m,numerical}=0.3776Re^{0.4636} \quad (12)$$

If numerical results are compared with experimental results, it can be seen that the Nusselt number predicted by equation (12) are about 4 percent higher than the Nusselt number predicted by equation (11).

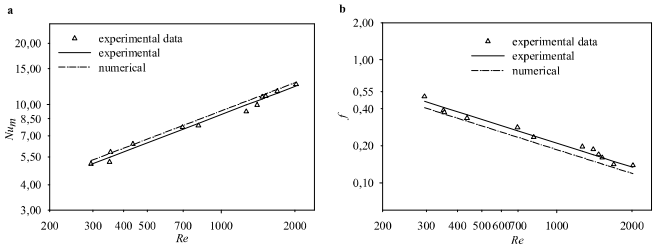

Figure 8 (**a**) the changing of average Nusselt number with Reynolds number; (**b**) the changing of average Darcy friction factor with Reynolds number

A single equation for average experimental Darcy friction factor representing data in laminar flow region is presented as follows:

$$f_{experimental}=17.66Re^{-0.6420} \quad (13)$$

The maximum deviation from the best-fit line for Eq. (13) is ±10.9 %. A single equation for numerically obtained average Darcy friction factor as a function of Reynolds number is presented as given below:

$$f_{numerical}=15.67Re^{-0.6420} \quad (14)$$

It is seen that the numerical results are approximately 11.3 % less than the experimental results. Equations (11)-(14) represent the experimental and numerical results for a range of Reynolds number from 295-2019.

CONCLUSIONS

Heat transfer and fluid friction for hydrodynamically and thermally developing three-dimensional steady laminar flow in a horizontal rectangular duct with constant bottom surface temperature were both experimentally and numerically investigated with the Reynolds number ranging from 295 to 2019 for $Pr\cong0.7$. The results of experimental data and numerical computations are presented in terms of average Nusselt number and average Darcy friction factor as a function of Reynolds number. Experimental results are compared with numerical results and it is observed that the experimental results are harmonious with numerical results. New engineering correlations are presented for the friction and heat transfer coefficients with nearly ±10.9 % and ±5 %, respectively. The present study is hoped to provide useful data for the design of thermal equipment.

ACKNOWLEDGEMENTS

This work was made possible through the financial support of the Unit of Scientific Research Projects of Gazi University in Turkey.

REFERENCES

[1] Shah, R.K., and London, A. L., *Laminar Flow Forced Convection in Ducts*, 1978, pp. 256-259, Academic Press Inc., New York.

[2] Kakaç, S., Shah, R.K., and Aung, W., *Handbook of Single-Phase Convective Heat Transfer*, 1987, Chapter 3, pp. 4, John Wiley and Sons, USA.

[3] Kakaç, S., and Liu, H., *Heat Exchangers Selection, Rating, and Thermal Design*, 2002, 2nd ed., pp. 81-127, CRC Press, USA.

[4] Zhang, L., Thermally developing forced convection and heat transfer in rectangular plate-fin passages under uniform plate temperature, *Numerical Heat Transfer Part A*, Vol. 52, 2007, pp. 549-564.

[5] Muzychka, Y.S., and Yovanovich, M.M., Laminar forced convection heat transfer in the combined entry region of non-circular ducts, *Journal of Heat Transfer*, Vol. 126, 2004, pp. 54-61.

[6] Chung, B.T.F., Zhang, Z.J., and Li, G., Thermally developing convection from Newtonian flow in rectangular ducts with uniform heating, *Journal of Thermophysics*, Vol. 7, No. 3, 1992, pp. 534-536.

[7] Aparecido, J.B., and Cotta, R.M., Thermally developing laminar flow inside rectangular ducts, *International Journal of Heat and Mass Transfer*, Vol. 33, No. 2, 1990, pp. 341-347.

[8] Beavers, G.S., Sparrow, E.M., and Magnuson, R.A., Experiments on hydrodynamically developing flow in rectangular ducts of arbitrary aspect ratio, *International Journal of Heat and Mass Transfer*, Vol. 13, 1970, pp. 689-702.

[9] Montgomery, S.R., and Wibulswas, P., Laminar flow heat transfer for simultaneously developing velocity and temperature profiles in ducts of rectangular cross section, *Applied Science Research*, Vol. 18, 1967, pp. 247-259.

[10] Sparrow, E.M., Analysis of laminar forced convection heat transfer in entrance region of flat rectangular ducts, *NACA Technical Note 3331*, 1955.

[11] Savino, J.M., and Siegel, R., Laminar forced convection in rectangular channels with unequal heat addition on adjacent sides, *International Journal of Heat and Mass Transfer*, Vol. 7, 1964, pp. 733-741.

[12] Kays, W., Crawford, M., and Weigand, B., *Convective Heat and Mass Transfer*, 2005, 4th ed., pp. 117-119, McGraw-Hill, Singapore.

[13] Leung, C.W., Chan, T.L., and Chen, S., Forced convection and friction in triangular duct with uniformly spaced square ribs on inner surfaces, *Heat and Mass Transfer*, Vol. 37, No. 1, 2001, pp. 19-25.

[14] Benedict, R.P., *Fundamentals of Temperature, Pressure and Flow Measurements*, 1977, 2nd ed., pp. 339-369, John Wiley & Sons, New York.

[15] Holman, J.P., *Experimental Methods for Engineers*, 2001, 7th ed., pp. 48-125, McGraw-Hill, New York.

[16] Çengel, Y.A., *Heat Transfer a Practical Approach*, 1998, pp. 372-380, McGraw-Hill, USA.

[17] Schlichting, H., and Gersten, K., *Boundary Layer Theory*, 2000, 8th ed., pp. 3-49, Springer, Germany.

[18] Incropera, F.P., and DeWitt, D.P., *Fundamentals of Heat and Mass Transfer*, 2002, 5th ed., pp. 917, John Wiley and Sons, USA.